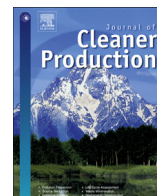




Contents lists available at ScienceDirect

Journal of Cleaner Production

journal homepage: www.elsevier.com/locate/jclepro

Production of fructose sugar from aqueous solutions: nanofiltration performance and hydrodynamic analysis

Siddhartha Moulik^a, Pavani Vadthya^a, Yamuna Rani Kalipatnapu^b, Sumana Chenna^b, Sridhar Sundergopal^{a,*}

^a Membrane Separations Group, Chemical Engineering Division, Indian Institute of Chemical Technology (IICT), Hyderabad 500007, India

^b Process Simulation and Control Group, Chemical Engineering Division, Indian Institute of Chemical Technology (IICT), Hyderabad 500007, India

ARTICLE INFO

Article history:

Received 20 July 2014

Received in revised form

22 November 2014

Accepted 26 December 2014

Available online xxx

Keywords:

Nanofiltration

Functionalized polyamide membrane

Fructose concentration

Hydrodynamic analysis

ABSTRACT

Nanofiltration (NF) is a rapidly advancing membrane technique for concentration of sugar and multi-valent salt solutions. The performance of indigenously synthesized functionalized polyamide (FPA) nanofiltration membranes of 150 and 250 molecular weight cut off (MWCO) was studied with respect to their ability to concentrate 2% (w/v) aqueous fructose with minimum losses of the sugar in permeate. Water flux and fructose retention properties of the NF membranes were compared to that of commercial reverse osmosis (RO) membranes. At an applied feed pressure of 10 bar, fructose rejection was found to be 94.14, 60.2 and 98.7% for FPA-150, FPA-250 and RO membranes, respectively. Hydrodynamic analysis was performed to study detailed fluid flow profile inside the membrane module to aid design of membrane systems. Economic estimation revealed that nanofiltration by FPA-150 membrane costs just 15.27% of that required by conventional evaporation for treating 1 m³/h fructose, owing to high flux combined with minimum sugar loss.

© 2015 Elsevier Ltd. All rights reserved.

1. Introduction

Fructose, a six-carbon monosaccharide, is a highly useful natural sweetener available in various food products including fruits, vegetables and honey. Compared to sugars like glucose and sucrose, crystalline fructose has a low glycemic index and requires low levels of insulin release into the blood stream for its metabolism. Concentrating the aqueous fructose solution is one of the important steps to facilitate subsequent crystallization during sugar production in the industry. A small quantity of this sugar gives relatively more sweetness than some of the other naturally occurring sugars viz., added starches, syrups and sweeteners resulting in high commercial value for crystalline fructose (Dolan et al., 2010). Concentrated fructose syrup is another commodity which is a source of instant energy while possessing additional functional properties over sucrose solutions such as high osmotic pressure and high solubility which prevents the formation of sugar crystals in food products (Kurup et al., 2005).

Concentration of sugar solutions and fruit juices is of prime importance as it reduces costs involved in packaging, storage and transport besides preventing microbial deterioration (Thanedgunbaworn et al., 2007). In the conventional process for production of crystalline sugar, the aqueous extract is concentrated by evaporation followed by crystallization. Evaporation is energy intensive owing to the phase change which requires high latent heat of vaporization (2260 kJ/kg). Development of a more economical process for separation of water from dilute sugars such as fructose constitutes the focus of this study. In this context, membrane processes could play a vital role as seen from previous studies carried out by researchers on osmotic distillation (Versari et al., 2004), nanofiltration (NF) (Seres et al., 2004), membrane distillation (Nene et al., 2002) and reverse osmosis (RO) for concentration of sugar syrups. Hogan et al., 1998 reported a hybrid process involving pre-concentration of the feed by RO followed by further concentration using osmotic distillation which produced a highly concentrated sugar product with significant reduction in processing cost. Vaccaria et al., 2005a, 2005b, proposed an integrated process combining microfiltration and crystallization for beet sugar processing. Warczok et al., 2004 reported a process based on NF to concentrate apple and pear juices at low pressures. A detailed description of membrane processes applied in fruit juice

* Corresponding author. Tel.: +91 40 27191394; fax: +91 40 27193626.

E-mail address: sridhar11in@yahoo.com (S. Sundergopal).

concentration has been reviewed by Jiao et al., 2004. Research data available in the literature on membrane-based concentration of sugar solution and fruit juice is presented in Table 1.

NF is a pressure driven membrane process which functions on the basis of steric and donnan effects (Aleixandre et al., 2011). NF has a wide scope of application for treatment of effluents coming from production of cheese (Nguyen et al., 2007), leather (Aleixandre et al., 2011), dyestuffs (Kim et al., 2005; Nouha et al., 2012) and textiles (Vishnu et al., 2008). The molecular weight cut off (MWCO) of NF, which ranges from 100 to 1000 Da, is suitable for effective rejection of sugar molecules. NF is more selective than UF and consumes lower energy than RO. These properties make NF potentially suitable in the sugar industry to save energy by reducing evaporator load during concentration of sugars like fructose (Warczok et al., 2004).

Accordingly, it is necessary to use Computational Fluid Dynamics (CFD) approach for evaluating the hydrodynamic scenario within the membrane module. Sarkar et al., 2012, reported CFD approach for finding the velocity and pressure profile within an ultrafiltration membrane module. In our previous study, a CFD approach has been reported to predict the hydrodynamic profile within the membrane bioreactor (Praneeth et al., 2014). A few studies were performed to understand the flow behavior inside the spacer incorporated NF modules using Computational Fluid Dynamics (CFD) (Ghidossi et al., 2006). Various experimental and theoretical studies were carried out to visualize fluid flow phenomena to optimize spacer configuration (Gerald et al., 2003). It was also evident that the presence of spacers enabled the direction of fluid flow to change periodically which consequently reduced concentration polarization and membrane fouling.

The objective of the present study is to investigate the use of a functionalized polyamide NF membrane for safe and economical concentration of aqueous fructose to produce crystalline fructose sugar. Influence of various operating conditions including feed pressure on membrane properties such as flux, % water recovery and % fructose rejection as well as a comparative study with TFC polyamide RO are reported. CFD approach is undertaken to evaluate the hydrodynamic characteristics within the NF module. Detailed economical analysis of evaporation and NF processes is presented.

2. Materials and methods

2.1. Materials

Fructose, isopropanol, polyvinyl alcohol (PVA), *m*-phenylene diamine (MPD), polyethersulfone (PES), glutaraldehyde (GA), hexane, dimethyl formamide (DMF), propionic acid, polyethylene glycol (PEG) and piperazine were purchased from Sigma–Aldrich, USA. Trimesoyl chloride (TMC) was obtained from AVRA Synthesis Pvt. Ltd., India. Citric acid, ethylenediamine tetraacetic acid (EDTA), NaOH and sodium metabisulphite (SMBS) for washing and storage

of the membranes were purchased from sd Fine Chemicals Ltd., Mumbai, India. Deionized water for preparing fructose solution was generated from the same RO system used for the experiments.

2.2. Membrane preparation

15% w/v of PES was mixed with 3% propionic acid in DMF solvent and the resultant polymer solution was de-aerated to remove air bubbles before casting on a nonwoven polyester fabric support using a doctor's blade to achieve the desired thickness followed by immersion in ice cold water bath. The PES substrate prepared by the phase inversion method was ultraporos in nature with an MWCO of 50 kDa (Swamy et al., 2013). To prepare polyamide NF membrane by interfacial polymerization, the PES substrate was soaked in 1% aqueous solution of piperazine for 1 min. Excess water was drained off and the substrate was then immersed in hexane bath containing 0.1% TMC for 30 s. The membrane was then heated in an oven at 110 °C for 5 min to obtain thermally crosslinked NF membranes of 400 MWCO. The NF membranes were functionalized by dip coating in 0.75 and 1.5% PVA solutions which were in turn prepared in deionized water at 90 °C that contained GA crosslinker in similar proportion with PVA, to finally obtain FPA NF membranes of four layered structures with 250 and 150 Da MWCOs, respectively. The process for preparing NF polyamide membrane by interfacial polymerization is illustrated in Fig. 1(a). The physical structure of FPA membrane post dip coating in PVA solution is represented in Fig. 1(b). Thickness profile, MWCO and functional groups of the four layered functionalized polyamide membrane are provided in Table 2. RO membrane was prepared by the same interfacial polymerization procedure wherein the aqueous reactant piperazine was replaced with MPD, but not subjected to any functionalization. The flat sheet membranes were prepared on a larger scale and assembled into spiral wound membrane (SWM) modules each with an effective area of 2.5 m² with the help of Permionics Membranes Pvt. Ltd., Vadodara, India.

2.3. Pore size measurement by bubble point method

The synthesized membrane was mounted on a sample chamber filled with isopropanol (surface tension 21.7 dyn cm^{−1}) and allowed to get wetted totally. Pure N₂ gas was introduced into the chamber with gradual increase in pressure. The bubble point pressure value, wherein the gas pressure overcame the capillary flow of the fluid within the largest pore to produce the first bubble, was noted. The pore size of the membrane was measured by following equation (Otero et al., 2008):

$$r_p = \frac{2\sigma}{\Delta P} \cos \theta \quad (1)$$

Table 1
Literature review on application of NF/RO membrane processes for the concentration of fruit/ sugar solution

Membrane type	Feed solution	Pressure (bar)	Flux (L/m ² h)	Rejection (%)	Reference
NF (AFC 80)	Pear juice	12	5.6	54	(Warczok et al., 2004)
NF (MPT-34)	Pear juice	12	1.4	74	
NF (AFC 80)	Apple juice	12	5.9	59	
NF (MPT-34)	Apple juice	12	1.8	92	
NF (MPT-34)	Fructose solution	12	2	64	(Bánvölgyi et al., 2009)
RO	Black current juice	30	6	99	
RO	Orange juice	20	11	–	
TFC RO	Xylitol solution	10	6	99.5	
NF		10	13	93	(Murthy et al., 2005)
NF (FPA-150)	Fructose solution	10	40.9	94.14	
RO		10	27.1	98.7	Present Work

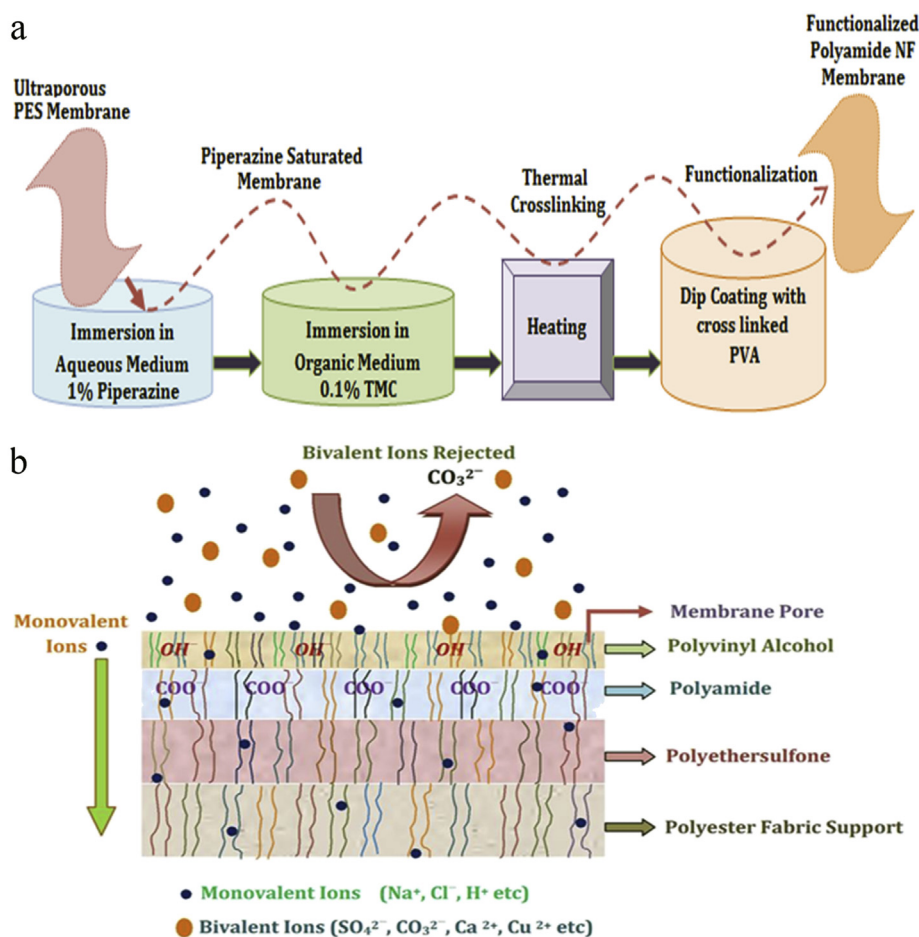


Fig. 1. (a) Flow diagram of NF Membrane preparation process (b) Physical structure of functional NF membrane depicting separation mechanism.

where, r_p is the pore radius (m), σ is the surface tension of liquid (N/m), θ is the contact angle between the two liquids and the membrane pore wall and ΔP is the pressure difference across the membrane (Pa).

2.4. Solute transport method

Aqueous solutions containing non-ionic macromolecules of PEG were used to test the flat sheet membranes. Initially, pure water flux was recorded and subsequently solute retention test was performed with increasing molecular weights of PEG (Singh et al., 1998). The initial feed solute concentration was noted and the solute separation was calculated using Eq. (2):

$$\%R = \left(1 - \frac{C_p}{C_f}\right) \times 100 \quad (2)$$

Where C_p and C_f are the corresponding solute concentration (mol/m^3) in permeate and feed.

2.5. Measurement of total dissolved solids (TDS)

In the measurement of total dissolved solids, a known volume of sample (10 mL) was taken on a pre-weighed empty glass Petri dish and the sample was heated slowly up to 105 °C in a sand bath

heater allowing the entire liquid in the Petri dish to evaporate. The weight of residual solids was then measured in a Sartorius electronic weighing balance to know the amount of dissolved solids present in 10 mL of sample. TDS was then calculated proportionately for 1 L of sample volume.

2.6. Description of NF/RO system

An in-house pilot scale NF/RO membrane system capable of incorporating both flat sheet and spiral wound membrane modules was utilized for the studies. A feed tank of 100 L capacity was installed for storage and supply of fructose solution followed by a polypropylene prefilter cartridge of 5 μm pore size that removes any suspended particulate matter which otherwise might choke or damage the membrane. A high pressure pump with a maximum capacity of 25 bar run by a 2 HP single phase motor was installed upstream of the membrane module. The feed pressure was maintained by regulating a restricting needle valve in the concentrate (reject) line. A coil type shell and tube heat exchanger was connected in order to bring down the temperature of retentate that gets heated up due to continuous pressurization and recirculation. Ice cold water was used as the cold stream in the heat exchanger to control reject temperature. Glass rotameters with metal floats were provided in both reject and permeate lines to measure feed and permeate flow rates. All the upstream connections were made of 1/

Table 2
Specifications of functionalized polyamide membrane

Membrane component	Thickness (μm)	MWCO (Da)	Functional group
Polyvinyl alcohol	5	150	–Nanoporous –OH
Polyamide	<0.1	250	–Nanoporous –CONH
Polyethersulfone	45	400	–Nanoporous
		50,000	–Ultraporous
Polyester fabric support	100	Macroporous	

2" o.d. stainless steel 316 piping to withstand high pressure whereas downstream connections were made of PVC braided tubing. The detailed process flow diagram of the NF/RO system for production of crystalline fructose is shown in Fig. 2.

2.7. Experimental procedure

2.7.1. Pure water flux

Prior to experiments with fructose feed, the membrane system was washed with deionized water until conductivity of permeate reached a value of at least 0.01 mS/cm. Then, a trial was carried out with deionized water at different feed pressures to study the effect of driving force on pure water flux. The deionized water was supplied from the feed storage tank and transported through the membrane module system by using the high pressure pump. The retentate was collected in a separate tank in order to maintain constant feed concentration. Feed pressure in the system was varied by throttling a needle valve in the retentate line to record permeate and retentate flow rates.

2.7.2. Trials with fructose feed

Initially, 2% w/v homogeneous fructose solution was prepared in 35 L of deionized water and transferred to the feed tank. After flushing out the deionized water present as dead volume in the system, the sugar solution was recycled back to the feed tank.

Recirculation was carried out under the actual operating pressure range of 3–10 bar rather than at atmospheric pressure. The needle valve in retentate line was slowly throttled to develop the desired operating pressure during which both retentate (concentrate) and permeate streams were continuously recycled to the feed tank until the flux of permeate was more or less constant and variation in feed fructose concentration was minimal. The initial total dissolved solids (TDS), conductivity and temperature of feed were recorded. Subsequently, the permeate line was taken out of the feed vessel and permeate sample was collected in a separate bucket. TDS was noted for every 500 mL of permeate sample collected. The reject stream was continuously cooled through the heat exchanger and recycled totally to the feed tank until maximum recovery of water in permeate was feasible. All the experiments were repeated thrice with cleaned membrane and fresh feed solution. Initial feed, average permeate and final concentrate samples were collected for analysis. Feed and permeate concentrations were measured by HPLC (SPINCO Laboratory Pvt. Ltd. Chennai, India) and TDS content was determined using sand bath heating technique. Finally, the system was cleaned and washed with deionized water to remove scales from the membrane surface and solutes that plugged the pores.

2.7.2.1. Rejection, flux and percentage recovery. The extent of concentration of the sugar by the membrane process is represented in terms of % rejection of TDS, i.e. fructose, which was calculated by Eq. (2). Flux (J) is the rate of permeate volume collected per unit membrane area:

$$J = \frac{V_i}{A \times t} \quad (3)$$

where, V_i is the volume of permeate (L), A is the membrane area (m^2) and t is the time of operation (h).

% Recovery is the % of feed volume that is obtained as permeate during the process which can be calculated as per the relation given below:

$$\% \text{Recovery} = \frac{Q_p}{Q_f} \times 100 \quad (4)$$

where, Q_p and Q_f are the flow rates of permeate and feed (m^3/s).

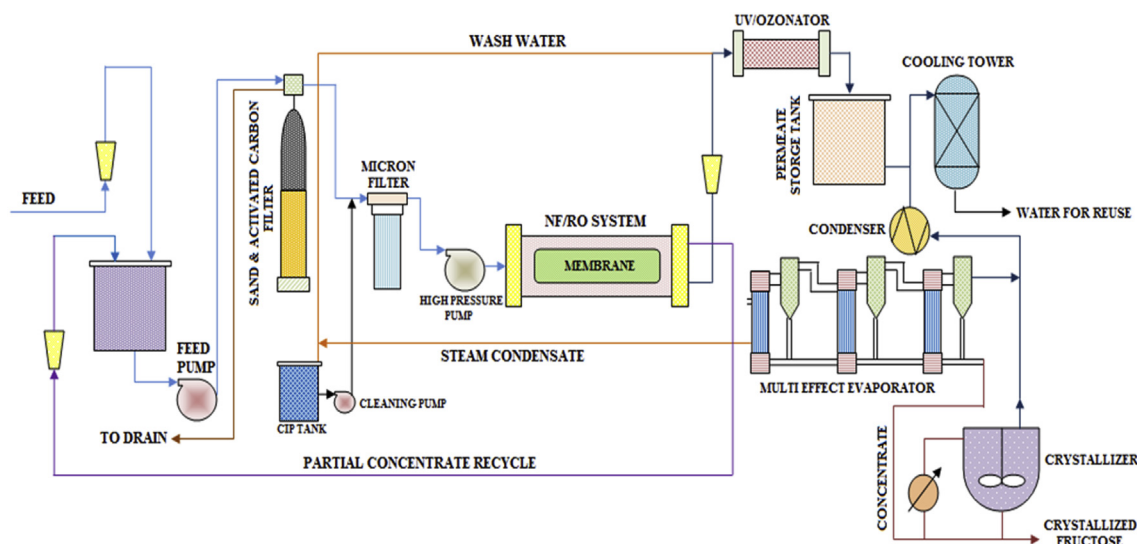


Fig. 2. Process Flow Diagram of membrane-based integrated process for fructose recovery.

2.8. Membrane fouling and its prevention

Membrane fouling can be caused by accumulation of suspended particulate matter, organic materials and microbial attack. Proper maintenance and monitoring of the membrane system is essential for better performance and life expectancy. The membranes were regularly washed with deionized water followed by 1% w/v citric acid for about 10 min to get rid of metal salt scales besides 1% w/v NaOH + 0.5% EDTA to remove stubborn organic foulants. To prevent biological fouling, the membranes were stored in aqueous sodium metabisulfite (0.5% w/v) after use. For experimentation with a fresh batch of feed, a water wash was provided to flush out the biocide sodium metabisulfite, before the membrane was exposed to fresh fructose feed.

2.9. Cost estimation

Cost comparison between NF and RO for a different application has been reported in one of our previous studies (Swamy et al., 2013). In the present case, a cost comparison between NF and evaporation is presented for concentrating aqueous fructose solution from 2 to 16 % at a production rate of 1 m³/h considering an operating period of 2 years. The costs are presented in US \$ assuming an average exchange rate of 55 Indian Rupees per US \$. A depreciation rate of 8% of the total capital investment (TCI) excluding site preparation cost, and an interest of 5% on TCI were also taken into account. The heat transfer area required for a multi-effect evaporator was estimated by the following equation:

$$UA\Delta T = mC_p\Delta T + m\lambda \quad (5)$$

where, U is the overall heat transfer coefficient (KJ/m²h K), A is heat transfer area required (m²), ΔT is the temperature difference (K), m is the feed flow rate (kg/h), C_p and λ , specific heat (kJ/kg K) and latent heat of vaporization of water (kJ/kg), respectively. Energy consumption for a positive displacement pump used in pressure driven membrane process was estimated as follows (Perry 1963):

$$E = \frac{Q_0 P_0}{1259.2 \eta \eta_m} \quad (6)$$

where E is the energy (kW), Q_0 is feed flow rate (m³/s), P_0 is feed pressure (Pa); η and η_m represent pump and motor efficiencies.

Energy consumption in evaporation process was estimated as follows:

$$E = mC_p\Delta T + m\lambda \quad (7)$$

2.10. Hydrodynamic analysis of SWM module

2.10.1. Specification of the SWM module geometry for computational domain and boundary conditions

The geometry of the membrane module was drawn using the finite element code COMSOL multi-physics 4.3b to evaluate the hydrodynamics and concentration profile within the membrane module. Fig. 3(a) (i) represents an SWM module in partly unwound state, in which the geometry of the module with spacer was constructed with a large number of flow cells, whereas, Figs. (ii) and (iii) represent detailed geometry of the computational domain. Fig. 3(b) depicts detailed meshed computational domain. The geometry of the membrane was drawn using the specific dimensions of the real module. In this study, four top and bottom filaments of the same diameter (0.0005 m) were considered for the simulation assuming non-woven structure of the spacer. The channel height, h_{ch} (m) was given by summing up the top and bottom filament diameters.

2.10.2. Governing equations and boundary conditions

2.10.2.1. Fluid flow. Continuity and momentum balance equations were solved assuming the fluid to be incompressible:

$$\nabla \cdot V = 0 \quad (8)$$

$$\rho \frac{DV}{Dt} = -\nabla P + \mu \nabla^2 V \quad (9)$$

where V is the velocity field (m/s), μ represents the fluid viscosity (Pa.s) and ρ is fluid density (kg/m³). Aqueous fructose solution was assumed to be the fluid. The channel Reynolds number is defined in Eq. (10) (Schock and Miquel, 1987):

$$Re_{ch} = \frac{u_{av} d_h}{\nu} \quad (10)$$

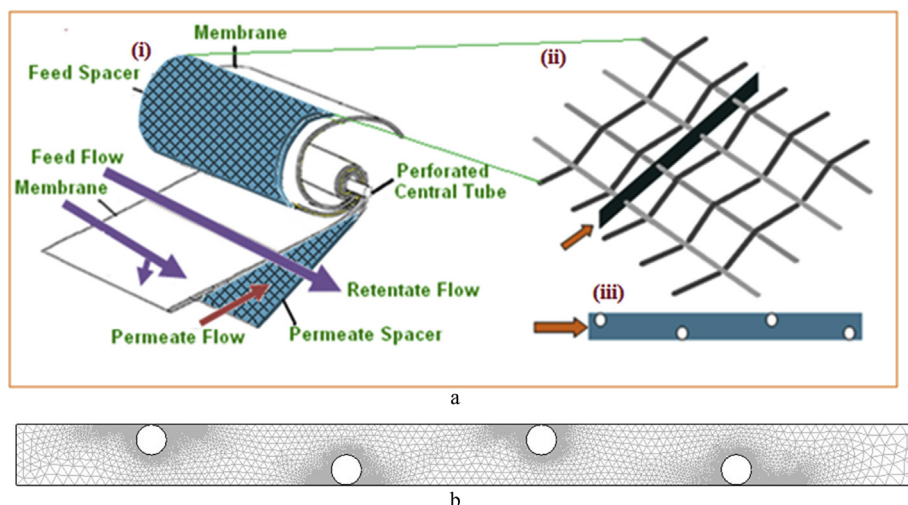


Fig. 3. (a) Computational domain for hydrodynamic analysis of NF/RO SWM module (b) Meshed computational domain of NF/RO channel.

where u_{av} is average velocity (m/s), d_h is the hydraulic diameter of the filament (m) and ν represents kinematic viscosity (m^2/s).

The hydraulic diameter (d_h) of the spacer filled channel is given by the following Eq. (11) (Saeed et al., 2012).

$$d_h = \frac{4\varepsilon}{\frac{2}{h_{ch}} + (1 - \varepsilon)S_{v,sp}} \quad (11)$$

The porosity (ε) and specific surface of the spacer ($S_{v,sp}$) (m^{-1}) (Saeed et al., 2012) is represented by

$$\varepsilon = 1 - \frac{\text{Spacer Volume}}{\text{Total Volume}} \quad (12)$$

$$S_{v,sp} = \frac{\text{Wetted surface of spacer}}{\text{Volume of spacer}} \quad (13)$$

At the inlet ($x = 0$) a fully developed laminar parabolic velocity profile was specified with an average velocity of $u_{in} = 0.1 \text{ ms}^{-1}$, a value kept constant with time. At the membrane surface the tangential velocity u_w (m/s) was set to zero. The permeate flux v_w (m/s) is linearly proportional to the difference between the high pressure applied within the channel and osmotic pressure formed on the membrane surface. The proportional coefficient is membrane permeability L_p ($\text{m}/\text{Pa}\cdot\text{s}$).

$$v_w = L_p(\Delta P - \Delta\pi) \quad (14)$$

Where, the TMP (ΔP) is defined as the difference between the local pressure on the feed side of the membrane and constant permeate pressure in the units of Pascal (Pa) whereas $\Delta\pi$ is the osmotic pressure (Pa) created by concentration polarization. The average flux in $\text{L}/\text{m}^2\text{h}$ was calculated by integrating the local permeate velocity v_w (m/s) over the channel length L (m) for both upper and lower membrane leaves in the spirally wound arrangement.

$$J = \frac{1}{L} \int_0^L v_w dx \quad (15)$$

2.10.2.2. Mass balance. The convection and diffusion equation (Eq. 16) was used to find out the fructose concentration in the channel:

$$u \frac{\partial c}{\partial x} + v \frac{\partial c}{\partial y} = D \left(\frac{\partial^2 c}{\partial x^2} + \frac{\partial^2 c}{\partial y^2} \right) \quad (16)$$

where the diffusion coefficient D (m^2/s), depends on concentration c (mol/m^3) and temperature T (K). At the inlet ($x = 0$), initial concentration of fructose was specified and concentration were constant with time. Condition of no diffusion ($D\delta C/\delta x = 0$) was applied on the outlet boundary. Insulation boundary condition was applied on the spacer surfaces. The convective flux of solute toward the membrane equals the sum of diffusive backward transport of the solute and the convective flux through the membrane.

$$\left(vC - D \frac{\partial c}{\partial y} \right) = vC(1 - R) \quad (17)$$

where, R is the rejection coefficient (Eq. 2).

A numerical solver, namely unsymmetric pattern multifrontal package (UMFPACK), was applied as a direct solver for appropriate numerical solution of stiff and non-stiff nonlinear boundary value problems. The study was carried out using a standard personal computer with the average simulation time being about 719 s.

3. Results and discussion

3.1. Hydrodynamic simulation

The primary aim of CFD simulation was to investigate the hydrodynamics inside the membrane module in order to explain the variation in performance under different parametric conditions. Fig. 4(a) shows the concentration profile inside the channel for FPA-250 membrane whereas Fig. 4(b) and (c) represent the velocity and pressure profiles inside the membrane channel at 10 bar feed pressure for FPA-150 membrane. From some previous studies (Shakaib et al., 2009), it is quite evident that major portion of the fluid flow in SWM module is in the main flow direction (X-direction). However, due to the presence of axial filaments, two distinct zones pertaining to flow attachment and separation were created near the wall. The inlet velocity of fructose solution was 0.1 ms^{-1} which increased to 0.26 ms^{-1} near the filament surfaces due to vigorous periodic disturbance in the flow. Velocity fluctuated in the range 0.12 – 0.19 ms^{-1} depending on the position of the spacers. It can be visualized that, at the intersection of the two filaments, fluid flow tends to move towards the top filament indicating flow reattachment and shifts away from the top filament as it moves ahead in the normal flow direction which reveals flow separation. Graphical representations of the variation in fructose concentrations at the lower membrane wall are shown in Fig. 5(a) and (b). Along the channel length, the concentration increased from 111 to $117.8 \text{ mol}/\text{m}^3$ and 111 – $123 \text{ mol}/\text{m}^3$ for FPA-250 and FPA-150 membranes, respectively. Increment in fructose concentration along the wall was found at 0.005 m and 0.012 m inside the channel, since the solute molecules at the wall intensively accumulate near the attachment point between the bottom filaments and the membrane. Fig. 6(a) and (b) represent the variation of permeate flux from the upper membrane layer along the channel length. As the spacers block the membrane surface, a decrease in total flux was observed at spacer positions of 0.002 and 0.009 m . However, total flux was found to increase at the end of the filaments.

3.2. Model validation

3.2.1. Variation of permeate flux with feed pressure

Effect of feed pressure (3–10 bar) on flux through FPA-250, FPA-150 and RO membranes is shown in Fig. 7. The simulated results are represented by symbols whereas the experimental data are shown in the form of different types of line graphs. As expected, the experimentally determined flux increased linearly from 16.23 to $45.22 \text{ L}/\text{m}^2\text{h}$ for FPA-250, 11.66 – $40.89 \text{ L}/\text{m}^2\text{h}$ for FPA-150 and 7.2 – $27.12 \text{ L}/\text{m}^2\text{h}$ in case of RO membrane, due to an increase in trans-membrane pressure gradient, which is the driving force for permeation in both NF and RO processes. Fig. 7 reveals a close resemblance of simulated values with experimental observations in case of all three membrane types. The considerable agreement between the two sets of results confirms the authenticity of the mathematical model.

3.3. Effect of feed pressure on % fructose rejection

Fig. 8 displays the performance of all three membranes in terms of fructose retention. With an increase in feed pressure from 3 to 10 bar, the rejection increased from 48.13 to 60.2% for FPA-250, 80.2 – 94.14% for FPA-150 and 85.1 – 98.7% for RO membrane (Table 1). Increasing rejection of fructose can be explained on the basis of solution-diffusion mechanism which governs mass transfer in both NF and RO processes (Murthy et al., 2005). Rising hydrostatic pressure results in enhanced sorption of water. The polar

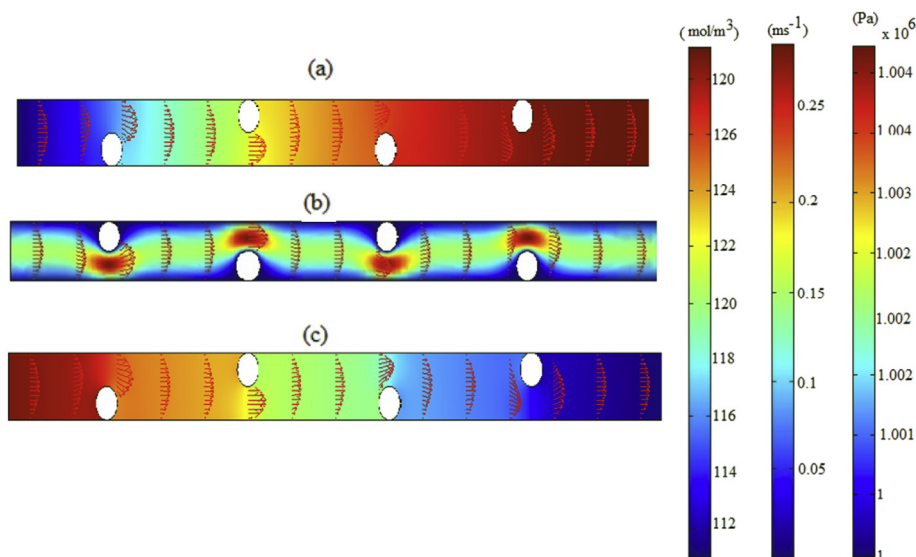


Fig. 4. Concentration, velocity and pressure profiles inside FPA-150 membrane at 10 bar pressure.

–CONH and –OH functional groups of the hydrophilic polyamide and PVA layers of the membrane attract water through hydrogen bonding whereas fructose molecules do not have much interaction with the membrane. Thus the flux of the sugar remains more or less constant as compared to increasing water transport, resulting in lower sugar concentration in permeate and subsequently greater solute rejection.

3.4. Variation of flux and water recovery with time

Fig. 9(a) and (b) were plotted after taking into consideration the standard deviation, to represent the variation in flux and % recovery with operating time for both NF and RO systems. All these experiments were carried out at two different feed pressures of 5 and 10 bar with initial feed volume of 35 L containing 2% fructose. The

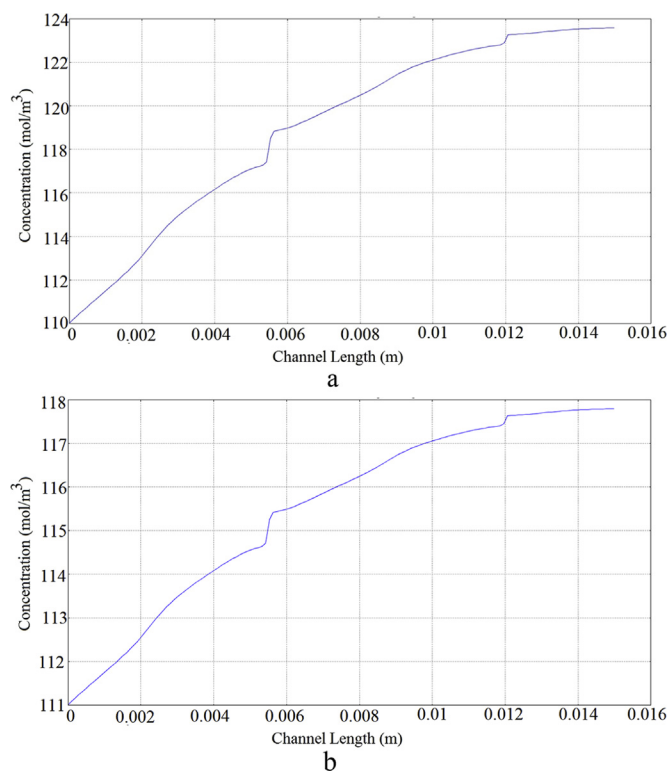


Fig. 5. Variation of concentration on the lower membrane wall for (a) FPA-150 and (b) FPA-250 at 10 bar pressure.

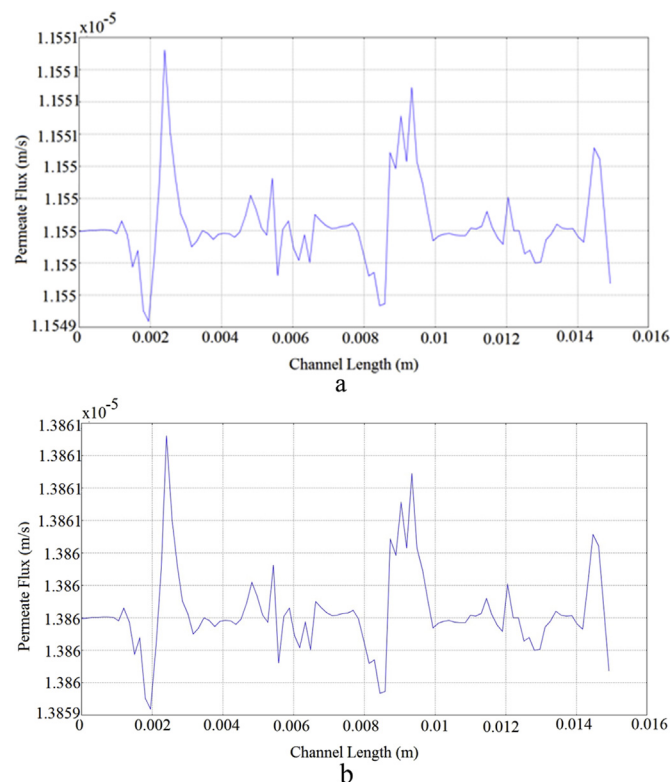


Fig. 6. Variation of permeate flux on upper membrane layer along the channel length (a) FPA-150 (b) FPA-250 at 10 bar pressure.

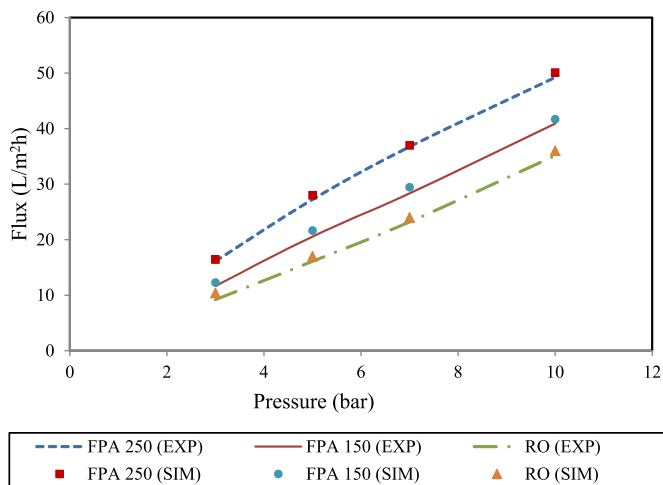


Fig. 7. Variation of permeate flux with feed pressure.

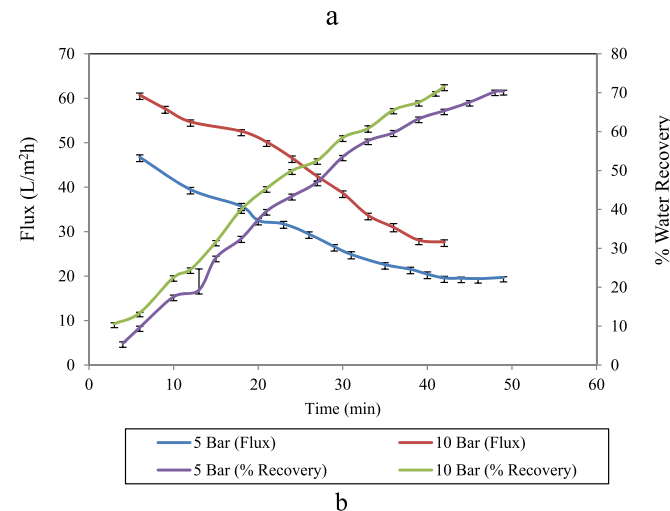
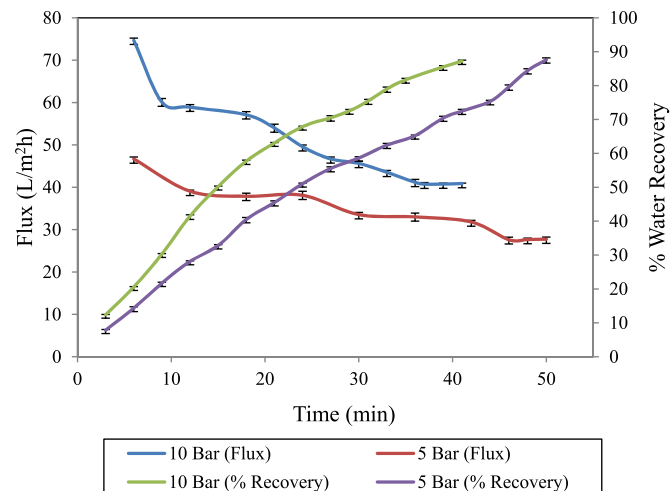


Fig. 9. Variation of flux and % water recovery with time for (a) FPA-150, (b) RO membranes.

pressure in any particular experimental trial was maintained constant. At a feed pressure of 10 bar, water recovery increased from 12.5 to 87.5% for FPA-150 and in the range 10.5–71% in case of RO, while the corresponding flux values decreased from 75 to 41 L/m²h and 61–27.12 L/m²h, respectively as illustrated in Fig. 9(a) and (b). With operating time, fructose solute molecules get increasingly retained owing to preferential permeation of water. This causes the osmotic pressure on the feed side to rise resulting in a decline in the driving force and consequently the flux as well. The accumulation of fructose molecules on the membrane surface enhances concentration polarization by the solute (sugar) followed by gradual fouling which leads to a decline in flux of the solvent, water (Das et al., 2006).

3.5. Economic estimation

Table 3 displays the capital and operating costs of NF and evaporation process for concentrating aqueous fructose solution from 2 to 16 % for a feed capacity of 1 m³/h considering 2 years of operating period.

3.5.1. Capital cost

3.5.1.1. Nanofiltration. The experimental results reveal an average flux of 40 L/m²hr through FPA-150 membrane to process fructose

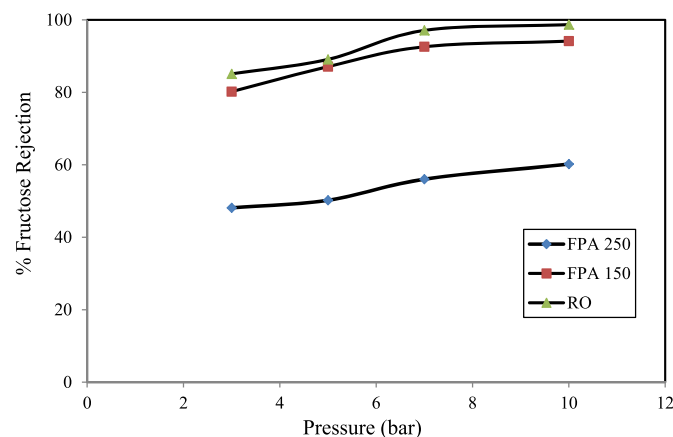


Fig. 8. Variation of % Rejection with feed pressure.

solution from 2 to 16 % at an operating pressure of 10 bar, which implies that a total membrane area of 25 m² is required to concentrate feed entering at a rate of 1 m³/h. The total area can be scaled up in the form of spiral wound membranes and distributed as 10 modules of 2.5" diameter × 40" length each having 2.5 m² effective area of FPA-150 membrane. Thus, the cost of the membrane and its housing (pressure vessel) are major contributors to capital investment which also includes the price of important components such as pumps, instrumentation and tanks as shown in Table 2. The total capital investment for the NF system comes to US\$ 12,964.

3.5.1.2. Evaporation. The capital cost estimation was carried out by a procedure similar to the one described in our previous study (Murthy et al., 2005). Detailed breakup of the cost for installation of a 4-effect evaporator system with all the necessary accessories is displayed in Table 2. The TCI for evaporation system was determined to be US\$ 13,200 which included an instrumentation cost of US\$ 3300.

3.5.2. Operating cost

3.5.2.1. Nanofiltration. Energy consumption of a high pressure positive displacement pump and membrane replacement cost are major contributors to the running cost in pressure driven

Table 3

Cost comparison between evaporation and NF methods for concentration of 1 m³/h fructose solution

Type of costs	Specification	Evaporation (US \$)	Nanofiltration (US \$)
Capital costs	System cost	4400	6364
	Pump costs	1100	2200
	Costs for site preparation	4400	2200
	Instrumentation	3300	2200
	Total	13,200	12,964
Operating Costs	Pumping	440	1106.6
	Steam(heating)	126,720	—
	Membrane replacement	—	2200
	Depreciation	1351.9	1182.5
	Sugar loss	5280	15,470
	Maintenance	275	550
	(Chemicals, Spares, etc.)		
	Total	134066.9	20509.1
	Cost (US\$/m ³)	10.15	1.55

membrane processes. The energy consumption for the high pressure pump was calculated by Eq. (6). The cost of operation was calculated on the basis of 1 m³/h of feed flow rate and a pressure of 10 bar, assuming the corresponding pump and motor efficiencies to be 0.6 and 0.7 (McCabe et al., 1993). The total operating cost includes cost of power consumption, sugar losses (US\$ 15,470), membrane maintenance, membrane replacement and depreciation (US\$ 1182.5) for a 2 year period of operation amounts to US\$ 20,509 indicating an expenditure of US\$ 1.55/m³ for processing 2% fructose solution to 10%.

3.5.2.2. Evaporation. Cost for operating a 4-effect evaporator in forward feed mode for fructose concentration was estimated to be US\$ 134066.9 for a 2 year period of operation (Murthy et al., 2005). Other operating costs include maintenance (US\$ 275), depreciation (US\$ 1351.9) and sugar losses (US\$ 5280). Thus the total operating cost of evaporation is US\$ 10.15/m³, which is six and half times higher than the running cost incurred in the NF process.

4. Conclusions

Both RO and NF membranes were found to be effective in concentrating aqueous fructose solution. FPA-150 NF membrane exhibited a fructose retention value of 94.14% which was comparable to that of the tighter RO membrane (98.7% rejection) at a higher flux of 40.9 L/m²h as against 27.7 L/m²h in case of RO at the same operating pressure of 10 bar. Thus, the comparable sugar retention coupled with higher flux makes NF an efficient alternative for fructose concentration. The membranes exhibited increasingly hydrophilic behavior at higher feed pressures as observed from improved water flux and fructose rejection owing to solution-diffusion mechanism in case of RO and NF besides the additional characteristic of pore compaction in case of NF. Hydrodynamic analysis enabled depiction of the detailed fluid flow profile inside the module including velocity, concentration and pressure profiles, besides helping in validation of experimental observations, which underlines the significance of CFD in performance prediction and design of commercial membrane systems. An economic estimation revealed the NF process to incur only about 15% of the expenditure involved in evaporation for concentrating 1 m³/h of aqueous fructose from 2 to 10%. For industrial production of crystalline fructose, an integrated process could be employed involving concentration of fructose up to 10–15% by NF beyond which evaporation can be employed for further concentration. Considering the potential

shown by experimental results and CFD simulation, the proposed NF process can be scaled up to serve as a cost-effective separation technology in the sugar industry.

Acknowledgement

The authors are thankful to Council of Scientific and Industrial Research (CSIR), New Delhi (CSC-0104), for granting funds for this project study under the MATES XII Five Year Plan Network Project.

References

- Aleixandre, M.V.G., Roca, J.A.M., Piá, A.B., 2011. Reducing sulfates concentration in the tannery effluent by applying pollution prevention techniques and Nanofiltration. *J. Clean. Prod.* 19, 91–98.
- Bánvölgyi, S., Horváth, S., Stefanovits-Bányai, É., Békássy-Molnár, E., Vatai, G., 2009. Integrated membrane process for blackcurrant (*Ribes nigrum* L.) juice concentration. *Desalination* 241, 281–287.
- Das, C., Patel, P., De, S., Gupta, S.D., 2006. Treatment of tanning effluent using nanofiltration followed by reverse osmosis. *Sep. Purif. Technol.* 50, 291–299.
- Dolan, L.C., Potter, S.M., Burdock, G.A., 2010. Evidence based review on the effect of normal dietary consumption of fructose on blood lipids and body weight of overweight and obese individuals. *Crit. Rev. Food. Sci.* 50, 889–918.
- Geraldes, V., Semiao, V., Pinho, M.N., 2003. Hydrodynamics and concentration polarization in NF/RO spiral wound modules with ladder-type spacers. *Desalination* 157, 395–402.
- Ghidossi, R., Veyret, D., Moulin, P., 2006. Computational fluid dynamics applied to membranes: state of the art and opportunities. *Chem. Eng. Process* 45, 437–454.
- Hogan, P.A., Canning, R.P., Peterson, P.A., Johnson, R.A., Mic, A.S., 1998. A new option: osmotic distillation. *Chem. Eng. Prog.* 94, 49–61.
- Jesus, D.F., Leite, M.F., Silva, L.F.M., Modesta, R.D., Matta, V.M., Cabral, L.M.C., 2007. Orange (*Citrus sinensis*) juice concentration by reverse osmosis. *J. Food Eng.* 81, 287–291.
- Jiao, B., Cassano, A., Drioli, E., 2004. Recent advances on membrane processes for the concentration of fruit juices: a review. *J. Food Eng.* 63, 303–324.
- Kim, T.H., Park, C., Kim, S., 2005. Water recycling from desalination and purification process of reactive dye manufacturing industry by combined membrane filtration. *J. Clean. Prod.* 13, 779–786.
- Kurup, A.S., Subramani, H.J., Hidajat, K., Ray, A.K., 2005. Optimal design and operation of SMB bioreactor for sucrose inversion. *Chem. Eng. J.* 108, 19–33.
- McCabe, W.L., Smith, J.C., Harriott, P., 1993. Unit Operations of Chemical Engineering, fifth ed. McGraw Hill, New York.
- Murthy, G.S., Sridhar, S., Sunder, M.S., Shankaraiah, B., Ramakrishna, M., 2005. Concentration of xylose reaction liquor by nanofiltration for the production of xylitol sugar alcohol. *Sep. Purif. Technol.* 44, 221–228.
- Nene, S., Kaur, S., Sumod, K., Joshi, B., Raghavarao, K.S.M.S., 2002. Membrane distillation for the concentration of raw cane-sugar syrup and membrane clarified sugarcane juice. *Desalination* 147, 157–160.
- Nguyen, M., Reynolds, N., Vigneswaran, S., 2007. By-product recovery from cottage cheese production by nanofiltration. *J. Clean. Prod.* 11, 803–807.
- Nouha, T., Ghazza, M., Emna, E., Amel, J., Patrick, D., Raja, B.A., 2012. Coupling microfiltration and nanofiltration processes for the treatment at source of dyeing-containing effluent. *J. Clean. Prod.* 33, 226–235.
- Otero, J.A., Mazarrasa, O., Villasante, J., Silva, V., Pradanos, P., Calvo, J.I., Hernandez, A., 2008. Three independent ways to obtain information on pore size distributions of nanofiltration membranes. *J. Membr. Sci.* 309, 17–27.
- Perry, J.H., 1963. Chemical Engineers' Handbook, fourth ed. McGraw Hill, New York, USA.
- Praneeth, K., Moulik, S., Pavani, V., Bhargava, S.K., Tardio, J., Sridhar, S., 2014. Performance assessment and hydrodynamic analysis of a submerged membrane bioreactor for treating dairy industrial effluent. *J. Hazard. Mater.* 274, 300–313.
- Saeed, A., Vuthaluru, R., Yang, Y., Vuthaluru, H.B., 2012. Effect of feed spacer arrangement on flow dynamics through spacer filled membranes. *Desalination* 285, 163–169.
- Sarkar, A., Moulik, S., Sarkar, D., Roy, A., Bhattacharjee, C., 2012. Performance characterization and CFD analysis of a novel shear enhanced membrane module in ultrafiltration of Bovine Serum Albumin (BSA). *Desalination* 292, 53–63.
- Schock, G., Miquel, A., 1987. Mass transfer and pressure loss in spiral wound modules. *Desalination* 64, 339–352.
- Seres, Z., Gyura, J., Eszterle, M., Vatai, G., 2004. Coloured matter removal from sugar-beet industry syrup by ultra and nanofiltration. *Acta Aliment.* 33, 119–127.
- Shakaib, M., Hasani, S.M.F., Mahmood, M., 2009. CFD modeling for flow and mass transfer in spacer-obstructed membrane feed channels. *J. Membr. Sci.* 326, 270–284.
- Singh, S., Khulbe, K.C., Matsuura, T., Ramamurthy, P., 1998. Membrane characterization by solute transport and atomic force microscopy. *J. Membr. Sci.* 142, 111–127.
- Swamy, B.V., Madhumala, M., Prakasham, Sridhar, S., 2013. Nanofiltration of bulk drug industrial effluent using indigenously developed functionalized polyamide membrane. *Chem. Eng. J.* 233, 193–200.

- Thanedgunbaworn, R., Jiratananon, R., Nguyen, M.H., 2007. Mass and heat transfer analysis in fructose concentration by osmotic distillation process using hollow fibre module. *J. Food Eng.* 78, 126–135.
- Vaccari, G., Sgualdino, G., Tamburini, E., Pezzi, G., Citterio, P., Verardi, R., Urbaniec, K., 2005b. New eco-friendly proposal for the crystallization of beet raw juice. *J. Clean. Prod.* 13, 447–460.
- Vaccaria, G., Tamburinia, E., Sgualdinoa, G., Urbaniecb, K., Klemes, J., 2005a. Overview of the environmental problems in beet sugar processing: possible solutions. *J. Clean. Prod.* 13, 499–507.
- Versari, A., Ferrarini, R., Tornielli, G.B., Parpinello, G.P., Gostoli, C., Celotti, E., 2004. Treatment of grape juice by osmotic evaporation. *J. Food Sci.* 69, 422–427.
- Vishnu, G., Palanisamy, S., Joseph, K., 2008. Assessment of field-scale zero liquid discharge treatment systems for recovery of water and salt from textile effluents. *J. Clean. Prod.* 16, 1081–1089.
- Warczok, J., Ferrando, M., López, F., Güell, C., 2004. Concentration of apple and pear juices by nanofiltration at low pressures. *J. Food Eng.* 63, 63–70.